Overexpression of AICD and Arc Drives APP Processing and Aggregate Formation in Drosophila

Noah Malhotra

Abstract:

Abnormal amyloid precursor protein (APP) processing, specifically cleavage through the amyloidogenic pathway creates amyloid-beta proteins that when oligomerized, causes brain damage and is a hallmark of Alzheimer's disease. Here, we examine how AICD and Arc expression affect APP localization and processing in Drosophila. Immunohistochemistry revealed that AICD overexpression induces Arc expression and leads to APP clustering and accumulation, which are not present in controls. Western blot analysis showed that Arc-GFP expression generates additional APP-related species, possibly by-products of APP proteolysis. This includes AICD, which drives the feed-forward loop in APP cleavage and Alzheimer's Disease. Furthermore, long-term memory (LTM) training increased APP cleavage in MBON-5β neurons, which in turn causes increased AICD and sAPP levels. These findings suggest that Arc and AICD are the main components in APP proteolysis, and memory related activity further drives the feed-forward loop in vivo.

Introduction:

The role of the amyloid cascade hypothesis has been the hallmark of Alzheimer's disease (AD) for many decades. Amyloid-beta plaques accumulate in the brain, leading to a series of events that cause neuronal damage[1]. Primarily, the plaques form neurofibrillary tangles made of the tau protein. While tau proteins are natural proteins that serve as a structural stabilizer in the brain, it can cause severe problems when hyperphosphorylated, such as disrupting neuronal communication and loss of brain function[2]. This is consistent with observed physical dysfunctions in patients affected by Alzheimer's disease, where obvious decreases in cognitive functions and memory recall are facilitated by an inability of neurons to communicate.
The creation of amyloid beta peptide (Aβ) is through a series of proteolysis processes on another protein, the amyloid precursor protein (APP)[3]. APP is a natural transmembrane protein that is broadly expressed during brain development. It supports neuronal proliferation and differentiation, and also is involved in synapse formation[4] When cleaved, an extracellular domain of the APP protein, sAPPα, is generated, taking on the role of neuroprotection and regulating

neuronal health[5]. Therefore, these proteolytic processes are naturally occurring without viral or bacterial intervention, and are also not subject to DNA mutations or irregularities. However, this cleavage is done through α-secretase in the middle of the fragment containing Aβ, which introduces the regular cellular functions found in humans without AD[6]. When APP is cleaved through the amyloidogenic pathway, the protein is cleaved by two other secretases, β-secretase (BACE1) at the N-terminus of the Aβ region and γ-secretase for the rest of the piece[7]. This is important because β-secretase cleavage causes Aβ to remain intact. Additional segments are created through this new proteolytic process, with sAPPβ being an inferior version of its alpha counterpart, a transmembrane protein with toxic properties to neuronal cells called C99, and crucially, the intracellular component AICD[8].

Once cleaved, the AICD fragment moves away from the membrane towards the center of the cell. There, it goes into the nucleus and becomes a transcription factor[9]. Inside the nucleus, important genes are upregulated, including the GSK-8B and BASE1. GSK-8B is a gene that codes for a crucial kinase important in tau phosphorylation regulation[10]. Previously mentioned, hyperphosphorylation of the tau protein produces neurofibrillary tangles that block synaptic signaling. BASE1 is the gene that encodes the β-secretase present in the proteolytic processes of the APP. A feed-forward loop is then created, where an upregulation of β-secretase causes an increase in cleavage, producing the harmful Aβ[11]. AICD production is also increased by the upregulation of the secretase.

The Activity-regulated cytoskeleton associated protein (Arc protein) is a protein vital in synaptic plasticity, neural learning, and memory formation. It is expressed in neuronal cells in response to activity across the synapses and is critical for Long-term potentiation (LTP) and memory consolidation. Studies have shown elevated Arc levels within brains of Alzheimer's patients. In drosophila tauopathy models, tau overexpression increases Arc1 expression, a fly homolog[12]. Moreover, Arc plays a role in a theory developed in the early 20th century, the Virus-like particle (VLP) theory. The protein contains a retrovirus-derived Gag domain, which allows it to create capsids contained with its own mRNA. This Arc mRNA capsid can be transferred between neurons, inducing endocytosis and mimicking viral infection in neuronal cells[13]. This ties in with AD because once tau protein becomes hyperphosphorylated, it disrupts a key process that keeps Arc mRNA levels in check called the nonsense-mediated mRNA decay. The end result is an

accumulation of Arc1 mRNA, causing overproductions of Arc and VLP formation. In brains without AD, Arc VLP regulates synaptic plasticity, but an overaccumulation of Arc VLP leads to synaptic weakening.

Methods:

Immunohistochemistry

See Table 1.

Dissections were performed on third instar *Drosophila melanogaster* larvae in 1× phosphate-buffered saline (PBS) without detergent. Brains were immediately transferred to 4% paraformaldehyde in phosphate buffer and fixed for a minimum of 1 hour at room temperature or overnight at 4 °C.

After fixation, brains were washed 3× with PBS containing 0.3% Triton X-100 (PBT) to permeabilize cell membranes. Samples were then blocked in 10% normal serum (goat or horse, as indicated by experiment) in PBT (PBTN) for 1 hour at room temperature to reduce nonspecific antibody binding.

Brains were incubated in primary antibody diluted in PBTN for at least 4 hours or overnight at 4 °C. After primary incubation, samples were washed three times for 25 minutes each in PBT. To minimize background during secondary staining, brains were re-blocked in PBTN for 30 minutes.
Fluorophore-conjugated secondary antibodies were applied in PBTN for a minimum of 4 hours or overnight at 4 °C. Final washes (3× in PBT, 25 minutes each) were conducted to remove unbound antibody. Brains were then mounted in Vectashield and imaged by confocal microscopy.

All confocal images were acquired using a Zeiss LSM 780 with a 63× Plan-Apochromat 1.4 NA DIC oil immersion objective. Images were taken using identical acquisition settings across experimental groups. Quantification of fluorescence signal was performed using ImageJ or Volocity software

Western blot

See Table 2.

Frozen *Drosophila melanogaster* heads were homogenized in 2× Laemmli sample buffer at 15 µL per head and boiled at 95 °C for 10 minutes to denature proteins. After brief centrifugation, equal amounts of protein (~20 µg per lane) were loaded onto 4–20% SDS-PAGE gels and electrophoresed using Tris-Glycine-SDS running buffer. Gels were initially run at 50 V for 5 minutes and then at 100–150 V for approximately 1 hour.

Following electrophoresis, proteins were transferred to nitrocellulose membranes in Tris-Glycine transfer buffer containing 20% methanol. For proteins larger than 80 kDa, SDS was included in the transfer buffer at 0.1% final concentration. Transfers were performed either at 100 V for 1–2 hours or overnight at 10 mA constant current in a cold room.

Membranes were briefly stained with Ponceau S (0.2% in 5% glacial acetic acid) to verify transfer quality, then rinsed and blocked in 3% BSA in TBST (20 mM Tris-HCl pH 7.5, 150 mM NaCl, 0.1% Tween-20) for 1 hour at room temperature.

Primary antibody incubation was performed overnight at 4 °C in blocking buffer. Blots were then washed 3–5 times for 5 minutes each in TBST and incubated with HRP-conjugated secondary antibodies for 1 hour at room temperature. After further washes, chemiluminescent detection was carried out using SuperSignal West Femto substrate. Signal was captured using a CCD camera-based ChemiDoc system (Bio-Rad). Band intensities were quantified using Image Lab software and normalized to total protein or a loading control.

Results

In order to examine the effects of AICD overexpression on APP localization and cleavage, immunohistochemistry (IHC) was performed using anti-APP and anti-Arc primary antibodies in control and AICD overexpressing samples of drosophila melanogaster brains (see Table 1 for specifics). The primary antibodies were conjugated with secondary antibodies, where APP is visualized with a Cy3 secondary (red) and Arc with a Cy5 secondary (blue). Samples were

imaged via confocal microscopy to assess protein localization in control and AICD samples.

Fig. 1A Posterior Brain Region - Sample Back 1

In control brains:

APP signaling through the red staining appeared to be distributed as expected adcross the tissue with no significant accumulation or localization. Arc signal was absent as expected in absence of AICD.

Quantification revealed that mean APP signal intensity decreased significantly in the AICD-overexpressing brains compared to control (from ~40 to ~18 arbitrary units), despite the structured reorganization observed (Fig.1E).

In AICD-overexpression brains:

Strong Arc signaling was observed throughout the central region of the tissue, which indicates a successful induction of Arc protein expression. Within these Arc-concentrated areas, however, APP staining showed further concentration and organization in structures. Notably, Region A displayed halos or rings surrounding cells that express Arc. In Region B, red fluorescence was observed in the peripheral regions with reduced Arc expression, a possible suggestion of aggregation of APP or accumulation of cleaved fragmentation.

Fig 1B. Posterior Brain Region - Sample Back 2

The control samples were consistent with Back 1 with diffuse APP staining but minimal Arc signal, and AICD samples displayed Arc accumulation in a bilobed structure. In Region C, Arc was robustly expressed throughout the dorsal lobe and also accompanied by an enhanced pericellular APP signaling. Moreover, in Region D, APP and Arc co-localized around a ventral subdomain, which suggests a distinct spatial regulation in subpopulations of Arc-expressing neurons.

Quantitative analysis showed a substantial drop in APP intensity in AICD-expressing brains,

from ~61 to ~33 units. This suggests a loss of global APP signal intensity in the posterior brain despite focal APP enrichment around Arc-expressing zones (Fig.1E).

Fig 1C. Anterior Brain Region - Sample Front 1

In control anterior brain sections, APP staining remained diffuse with little detectable Arc expression. In contrast, AICD-overexpressing brains showed distinct Arc-positive neuronal clusters. In Region E, Arc signal was confined to a discrete circular structure, surrounding APP signal appeared enriched, suggesting localized APP accumulation near Arc-expressing domains .

Quantification confirmed a striking increase in APP signal intensity, from ~25 units in control brains to ~54 in AICD-overexpressing samples. This supports the visual observation of Arc-guided APP enrichment in the anterior brain (Fig.1E).

Fig 1D. Anterior Brain Region - Sample Front 2
Control samples exhibited low APP intensity with no distinct structural organization. In AICD-overexpressing brains, a well-defined Arc-positive region emerged in the anterior domain. In Region F, APP fluorescence appeared enhanced and layered along the Arc-expressing structure. A notable detail is that the APP signal was sharply defined at the boundaries of Arc accumulation, suggesting that Arc expression may contribute to subcellular partitioning or trafficking of APP.

Quantitative data revealed a comparable increase in APP intensity, rising from ~22 in control to ~55 in the experimental group. This aligns with the anterior-specific APP elevation observed in confocal imaging and suggests region-dependent effects of AICD overexpression on APP distribution (Fig.1E).

Conclusion:

Consistently observed across all imaged brain regions, AICD overexpression induced Arc protein expression and was associated with a redistribution of APP signal. However, AICD-expressing brains exhibited Arc-dependent APP clustering, pericellular ring formation and regional

accumulation, which are in contrast to the diffuse APP staining in controls.

WB 1:

To assess whether Arc-GFP expression affects APP protein levels and cleavage, we performed Western blotting on lysates from control (OK107) and Arc-GFP–expressing Drosophila brains. Samples were treated with an anti-APP (-80) antibody (1:1,000) and visualized using an anti-chicken secondary antibody (1:10,000).
In control samples, a single faint band was detected at approximately 130 kDa, which corresponds with full-length APP. No additional bands were visible, which indicates expected minimal APP processing (See Fig. 2A).
In contrast, brains expressing Arc-GFP exhibited multiple distinct bands. The 130 kDa band was clearly more intense, which indicates an increase in full-length APP levels. However, a second molecular band at a higher weight, ~180 kDa, was also observed in the Arc-GFP condition, potentially representing a protein complex between APP and Arc-GFP or APP oligomerization.

Two additional lower-molecular-weight bands were identified:

A ~50 kDa band, which may represent a cleaved APP C-terminal fragment (e.g., AICD) possibly stabilized by interaction with Arc-GFP.

A ~25 kDa band, consistent with the expected size of Arc-GFP alone.

These bands were absent in control lanes, supporting their specificity to Arc-GFP expression.

Quantification of band intensities revealed that Arc-GFP expression reduced full-length APP levels (0.4 a.u. vs. 1.0 a.u.) and increased AICD signal (1.5 a.u. vs. 0.2 a.u.) compared to control. These results indicate enhanced cleavage of APP under Arc-GFP conditions. No significant signal was observed for intermediate cleavage fragments in the control group. A ~25 kDa band, consistent with Arc-GFP alone, was detected exclusively in the Arc-expressing group (see Fig. 2B).

Conclusion:

Together, these findings indicate that Arc-GFP expression increases APP levels and is associated with the appearance of additional APP-related species, including a potential high molecular weight complex and cleaved products. These results suggest that Arc-GFP does indeed alter APP processing in the Drosophila brain.

WB 2:
To investigate whether Arc1 expression affects APP processing in MBON-5β neurons, we performed Western blot analysis on fly brain samples expressing UAS.Arc1 under the control of the 5b and OK107 drivers. Protein lysates were probed with an anti-APP antibody to evaluate differences in full-length APP and its cleavage products.
Distinct bands were observed at ~130–140 kDa, which corresponds to full-length APP, as well as at ~100 kDa and ~30–35 kDa, representing soluble APPα/β (sAPP) and the APP intracellular domain (AICD) respectively. Arc1-overexpressing flies exhibited a notable reduction in the full-length APP band and an increase in AICD and higher-molecular-weight APP complexes (~180 kDa) compared to the control, which suggests an increase in cleavage (see Fig. 3A). Quantification of band intensities revealed that Arc1 overexpression reduced full-length APP levels (0.7 a.u. vs. 1.0 a.u.) and increased AICD/RFP signal (1.25 a.u. vs. 0.45 a.u.) compared to control. sAPP levels were modestly elevated (1.0 a.u. vs. 0.5 a.u.), and the ~180 kDa APP cluster band showed a pronounced increase under Arc1 expression (see Fig. 3B). These results indicate that Arc1 may promote APP cleavage or influence APP trafficking and complex formation within MBON-5β neurons, potentially altering downstream signaling pathways implicated in neurodegenerative processes.

Discussion:

The study demonstrates that Arc and AICD overexpression does indeed have a significant influence on APP processing and distribution seen in samples of transgenic drosophila brains.

IHC analysis revealed that AICD induces Arc protein expression across multiple different brain regions, and along with it a redistribution of APP signaling. Brains expressing AICD exhibited Arc-dependent APP clustering, which are unlike the diffuse APP staining observed in controls. Additionally, formation of organized structures and accumulation suggest that AICD may modulate synaptic membrane-associated trafficking of APP, and is actively involved in

increasing APP cleavage rates and continuing the feed-forward loop.

Western blot analysis showed that Arc-GFP expression in drosophila brains leads to the emergence of additional APP-related bands. These bands include a ~180 kDa band, which
potentially correlate to APP-Arc complexes or multiple APP oligomerized together. A lower band was also present, and observed to be consistent with AICD. These changed were not present in control brains, which indicates that Arc-GFP facilitates its proteolytic cleavage of stabilization of its fragments.

Further supporting this, Western blotting of MBON-5β neurons with long-term memory (LTM) training revealed that compared to untrained controls, brains from flies trained with LTM exhibited increased levels of APP cleavage products. This includes higher levels of AICD and sAPP, but interestingly as well as the appearance of ~180 kDa APP clusters seen in Western blot 1. These changes were not observed in 5β brains from flies without LTM training, however, which suggests that memory retrieval functions and cognitive processes may increase APP cleavage.

The findings suggest a model in which Arc and AICD play huge roles in the pathology of Alzheimer's disease, specifically in continuing the feed-foward loop that induces APP cleavage and further amyloid-beta production.

Figures:

Table 1. Created with Matplotlib
Table 2. Created with Matplotlib

Experiment	Genotype(s)	Blocking Serum	Primary Antibodies	Secondary Antibodies
IHC Round 1	OK107 vs. OK107 > UAS-Arc	Horse	anti-APP (-20) (1:500), anti-Arc (1:500)	Cy3 anti-chicken (1:500), Cy5 anti-rabbit (1:400)

Experiment	Genotype(s)	Primary Antibody	Dilution (Primary)	Secondary Antibody	Dilution (Secondary)
WB Exp 1	OK107 vs. Arc-GFP	αAPP (-80)	1:1,000	α-chicken HRP	1:10,000
WB Exp 2	5b no LTM vs. 5b LTM	αAPP (-20)	1:2,000	α-chicken HRP	1:2,000

Fig 1A.

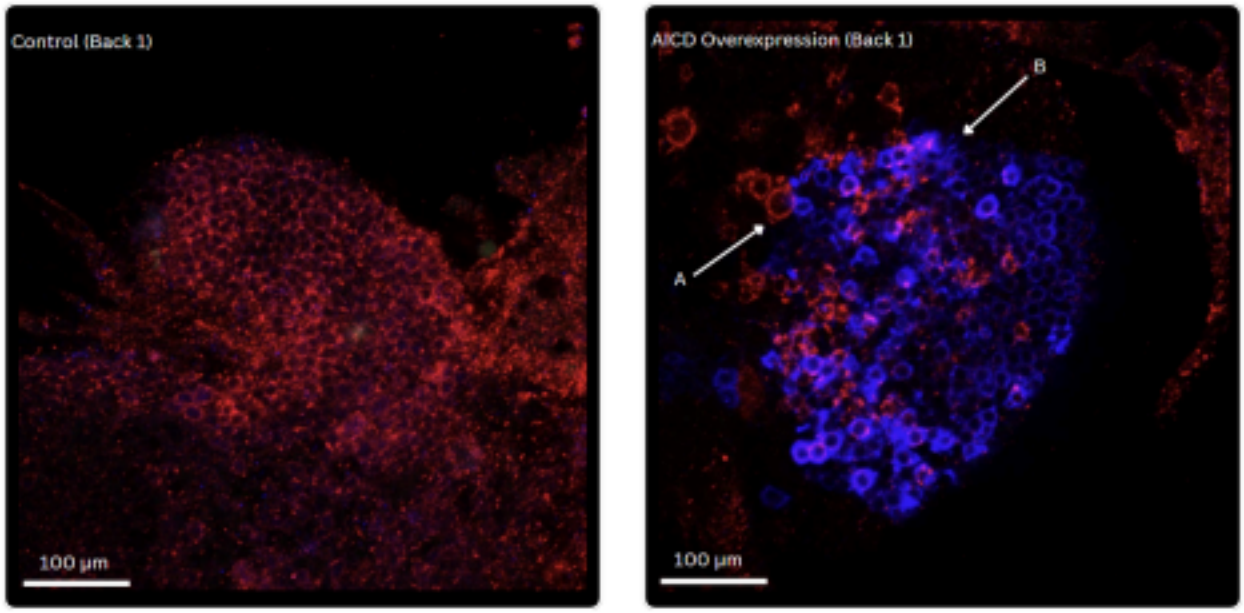

Fig. 1B

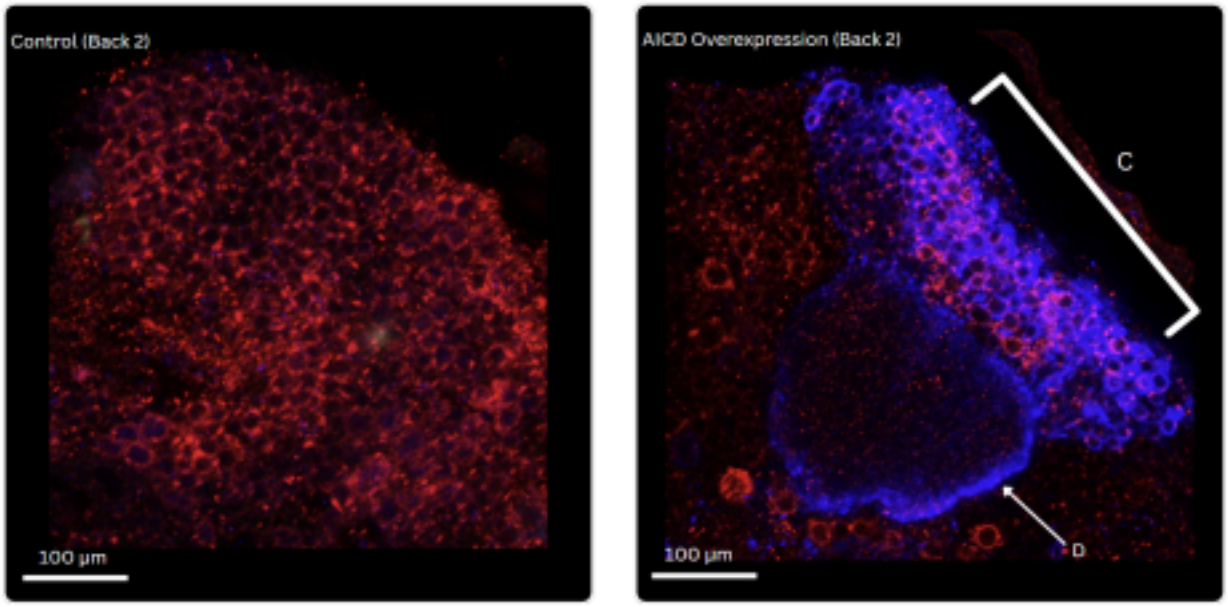

Fig. 1C

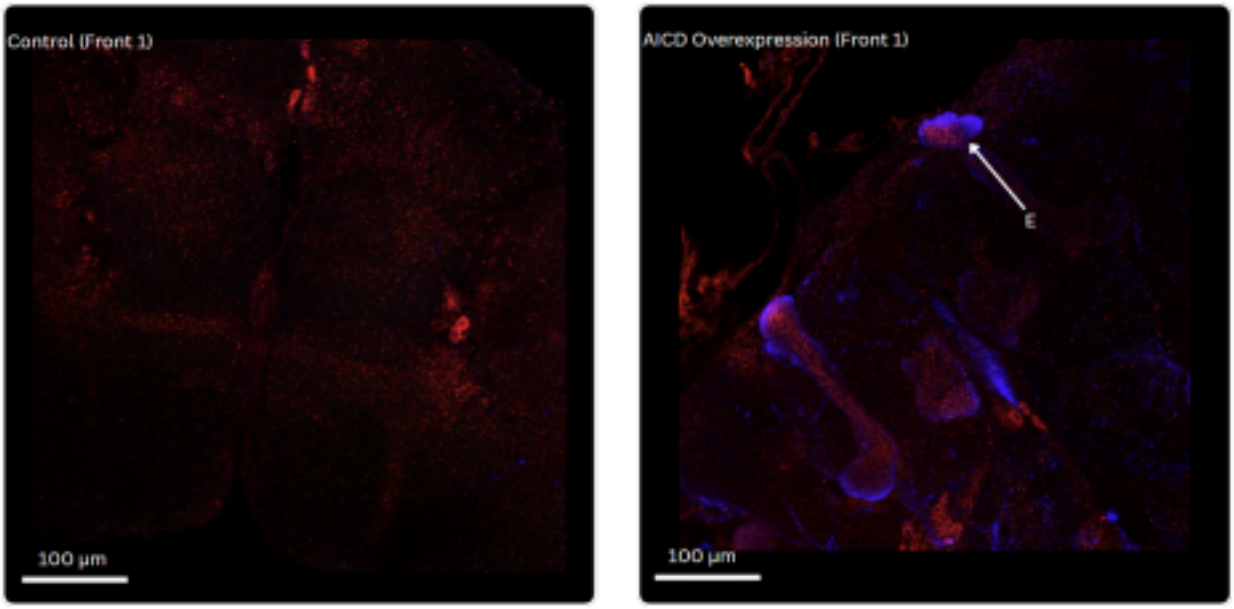
Control (Front 1)
100 µm
AICD Overexpression (Front 1)
E
100 µm

Fig. 1D

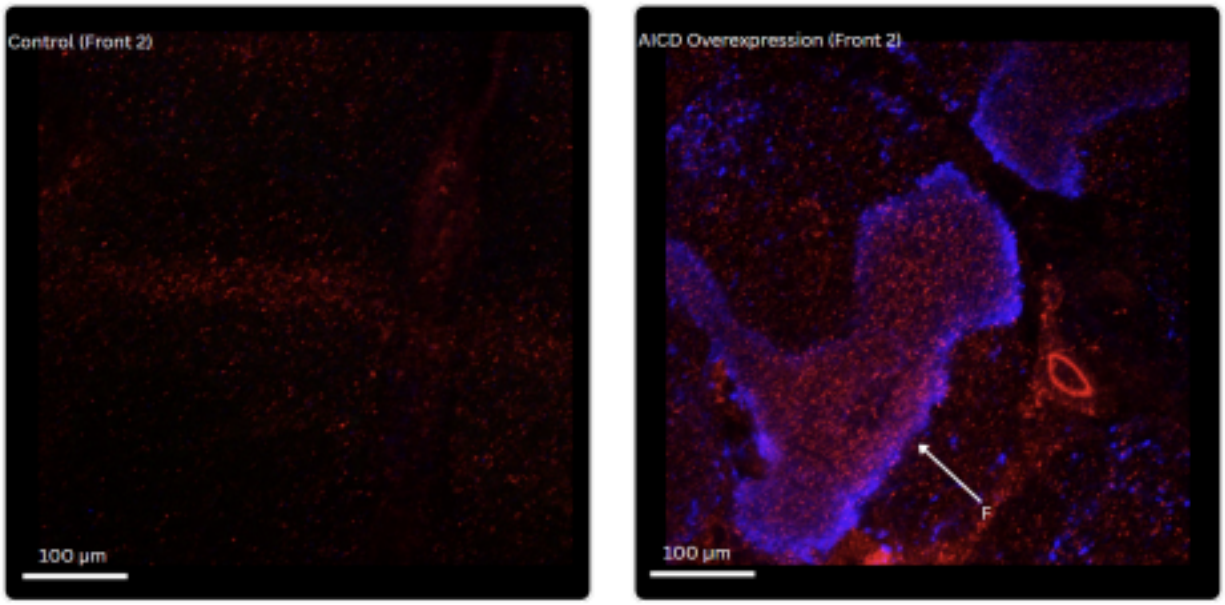
Control (Front 2)
100 µm
AICD Overexpression (Front 2)
F
100 µm

Fig. 1E

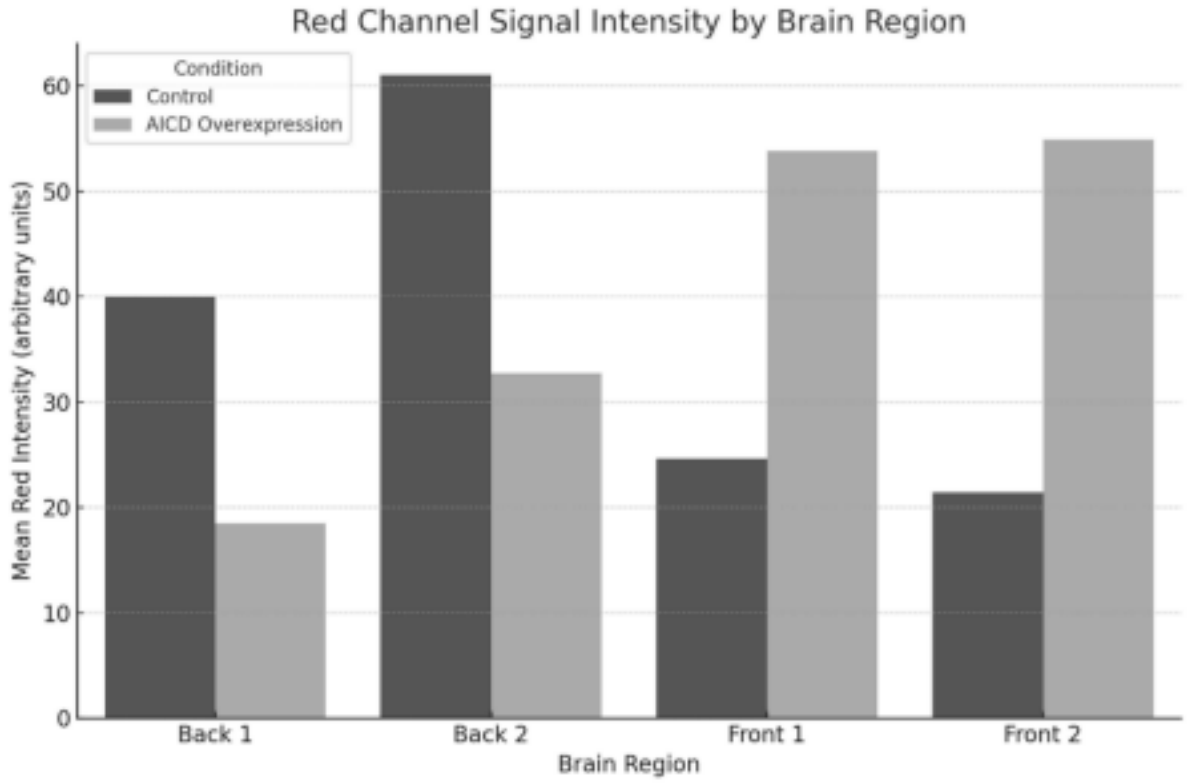
Red Channel Signal Intensity by Brain Region
Condition
Control
AICD Overexpression
Mean Red Intensity (arbitrary units)
0
10
20
30
40
50
60
Back 1
Back 2
Front 1
Front 2
Brain Region

Fig. 2A

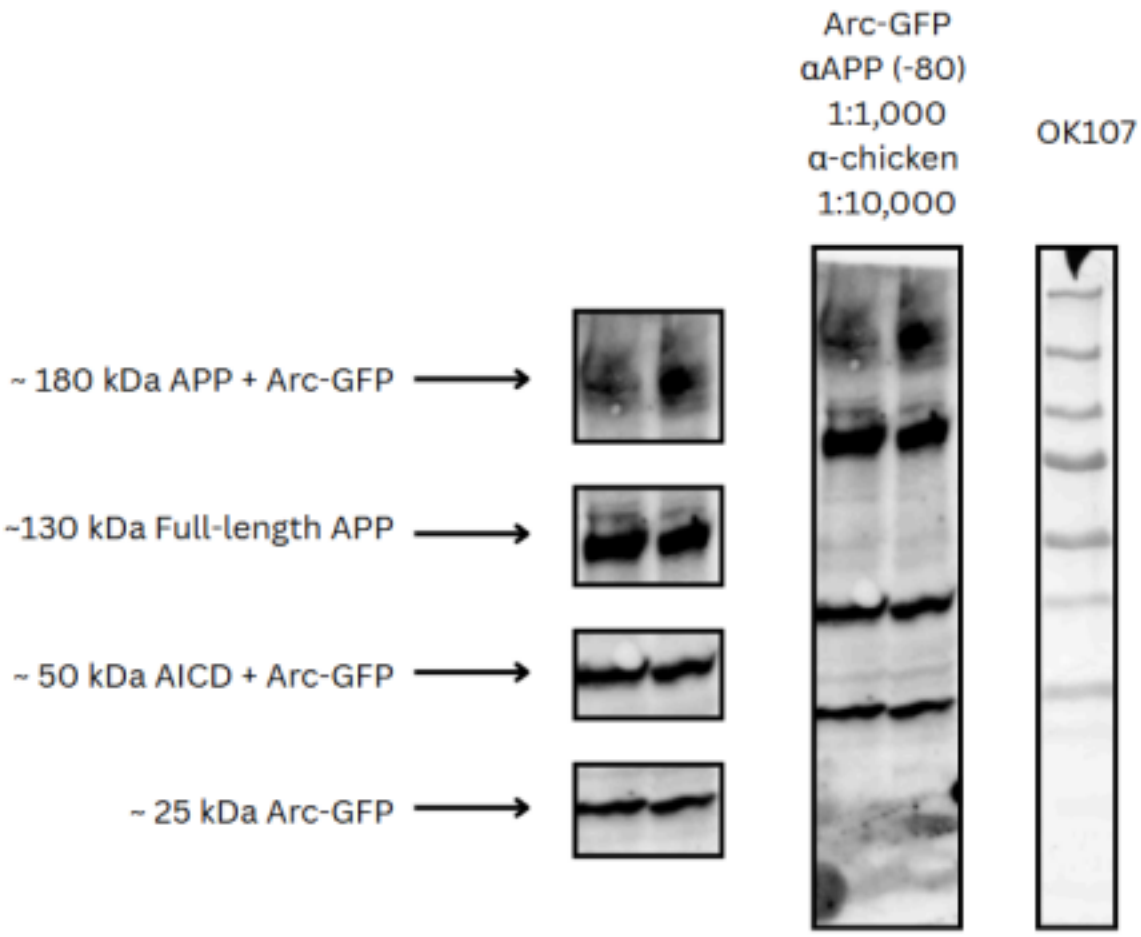
Arc-GFP
αAPP (-80)
1:1,000
α-chicken
1:10,000
OK107
~ 180 kDa APP + Arc-GFP
~130 kDa Full-length APP
~ 50 kDa AICD + Arc-GFP
~ 25 kDa Arc-GFP

Fig. 2B

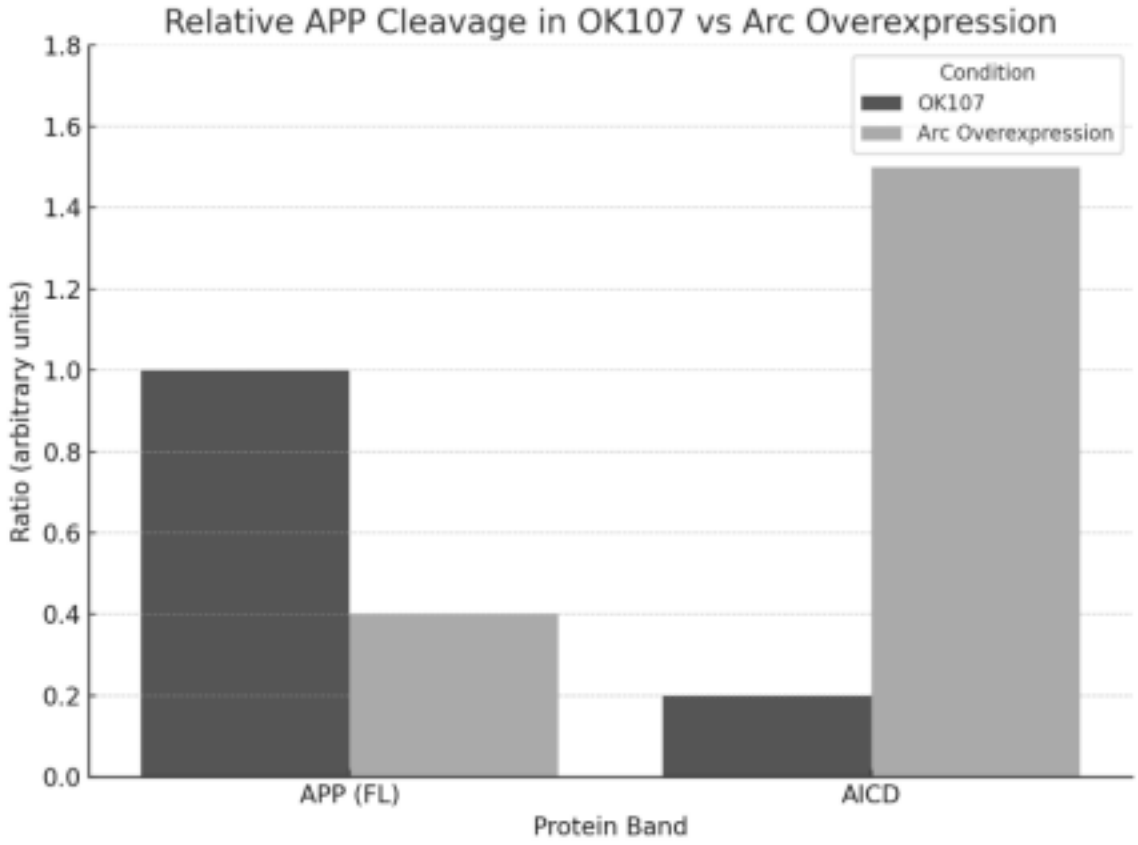
Relative APP Cleavage in OK107 vs Arc Overexpression
Condition
OK107
Arc Overexpression
Ratio (arbitrary units)
1.8
1.6
1.4
1.2
1.0
0.8
0.6
0.4
0.2
0.0
APP (FL)
AICD
Protein Band

Fig. 3A

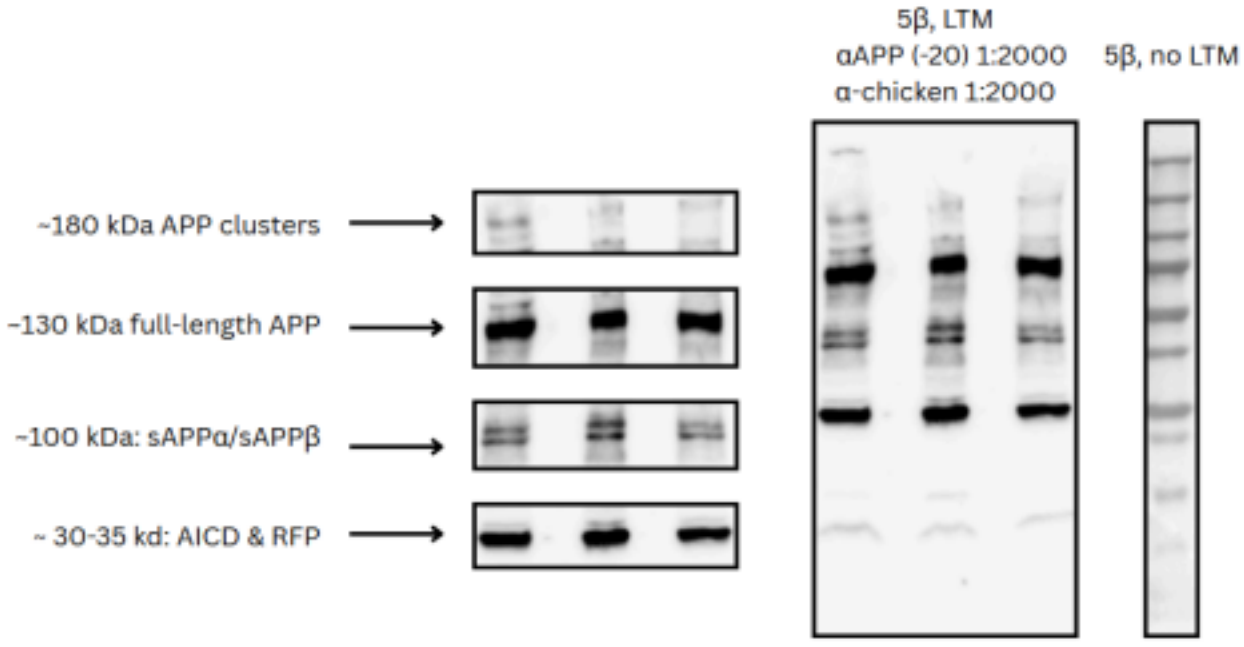
5β, LTM
αAPP (-20) 1:2000
α-chicken 1:2000
5β, no LTM
~180 kDa APP clusters
~130 kDa full-length APP
~100 kDa: sAPPα/sAPPβ
~ 30-35 kd: AICD & RFP

Fig. 3B

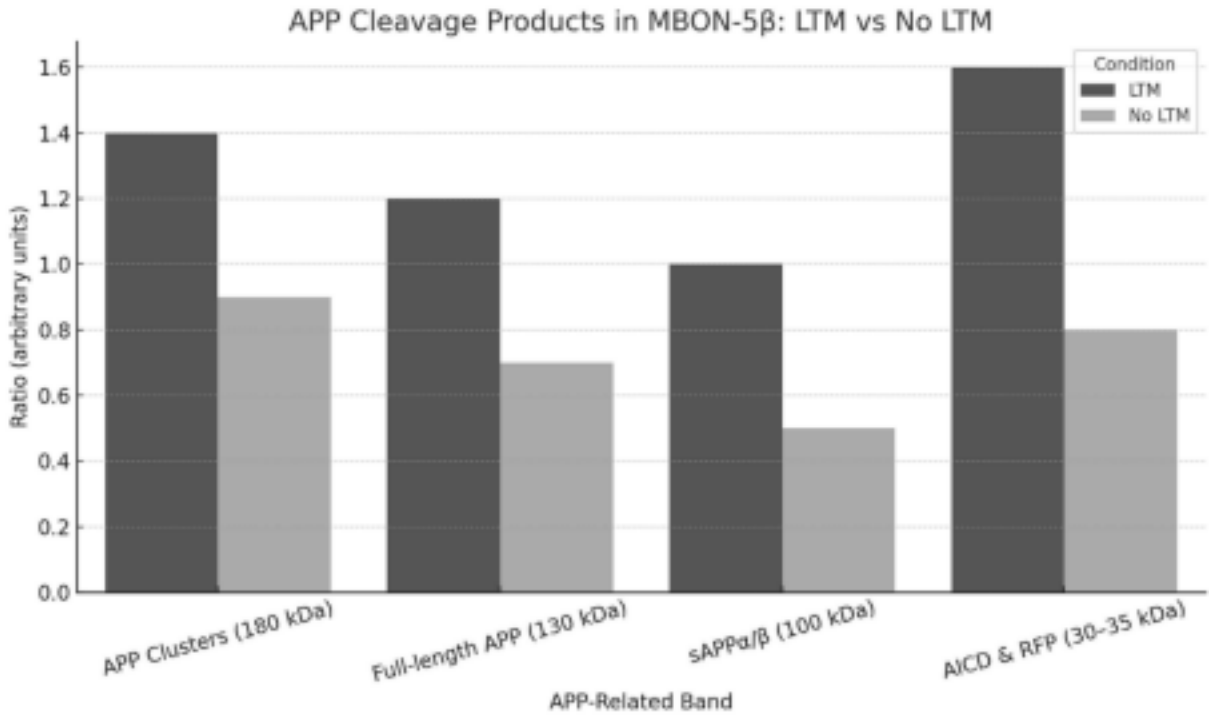

References:

1. Golde, Todd E et al. “Targeting Abeta and tau in Alzheimer's disease, an early interim report.” Experimental neurology vol. 223,2 (2010): 252-66. doi:10.1016/j.expneurol.2009.07.035

2. National Institute on Aging. What Happens to the Brain in Alzheimer’s Disease? U.S. Department of Health and Human Services, 22 May 2024, www.nia.nih.gov/health

3. Chen, Gf., Xu, Th., Yan, Y. et al. Amyloid beta: structure, biology and structure-based therapeutic development. Acta Pharmacol Sin 38, 1205–1235 (2017). https://doi.org/10.1038/aps.2017.28

4. Zheng, H., Koo, E.H. Biology and pathophysiology of the amyloid precursor protein. Mol Neurodegeneration 6, 27 (2011). https://doi.org/10.1186/1750-1326-6-27

5. Nhan, Hoang S et al. “The multifaceted nature of amyloid precursor protein and its proteolytic fragments: friends and foes.” Acta neuropathologica vol. 129,1 (2015): 1-19. doi:10.1007/s00401-014-1347-2

6. Masashi Asai, Chinatsu Hattori, Beáta Szabó, Noboru Sasagawa, Kei Maruyama, Sei-ichi Tanuma, Shoichi Ishiura, Putative function of ADAM9, ADAM10, and ADAM17 as APP α-secretase, Biochemical and Biophysical Research Communications, Volume 301,

Issue 1, 2003, Pages 231-235, ISSN 0006-291X.

7. Hur, JY. γ-Secretase in Alzheimer's disease. Exp Mol Med 54, 433–446 (2022). https://doi.org/10.1038/s12276-022-00754-8

8. Orobets KS, Karamyshev AL. Amyloid Precursor Protein and Alzheimer's Disease. International Journal of Molecular Sciences. 2023; 24(19):14794. https://doi.org/10.3390/ijms241914794

9. Müller, Thorsten et al. "The amyloid precursor protein intracellular domain (AICD) as modulator of gene expression, apoptosis, and cytoskeletal dynamics-relevance for Alzheimer's disease." Progress in neurobiology vol. 85,4 (2008): 393-406. doi:10.1016/j.pneurobio.2008.05.002

10. Chang, Keun-A et al. "Phosphorylation of amyloid precursor protein (APP) at Thr668 regulates the nuclear translocation of the APP intracellular domain and induces neurodegeneration." Molecular and cellular biology vol. 26,11 (2006): 4327-38. doi:10.1128/MCB.02393-05

11. Doig, Andrew J. "Positive Feedback Loops in Alzheimer's Disease: The Alzheimer's Feedback Hypothesis." Journal of Alzheimer's disease : JAD vol. 66,1 (2018): 25-36. doi:10.3233/JAD-180583

12. Schulz, Lulu et al. "Tau-Induced Elevation of the Activity-Regulated Cytoskeleton Associated Protein Arc1 Causally Mediates Neurodegeneration in the Adult Drosophila Brain." Neuroscience vol. 518 (2023): 101-111. doi:10.1016/j.neuroscience.2022.04.017

13. Ashley, James et al. "Retrovirus-like Gag Protein Arc1 Binds RNA and Traffics across Synaptic Boutons." Cell vol. 172,1-2 (2018): 262-274.e11. doi:10.1016/j.cell.2017.12.022